PHYSICAL REVIEW B VOLUME 10, NUMBER 8 15 OCTOBER 1974

Warm and hot carriers in silicon surface-inversion layers*

Karl Hess† and C. T. Sah
Department of Electrical Engineering and Materials Research Laboratory, University of Illinois, Urbana, Illinois 61801
(Received 23 January 1974)

A study of the hot-carrier effects for electrons in silicon inversion layers is reported. Measurements of the warm-electron coefficient β at 77 °K give -2×10^{-8} cm^2/V^2 in the ⟨110⟩ and -5×10^{-8} cm^2/V^2 in the ⟨100⟩ direction on a (110) silicon surface. A theory of β is given for the two-dimensional carrier gas model. The two-dimensional Boltzmann equation is solved in the diffusion approximation. Explicit results for the distribution function are given for scattering of the electrons by acoustic phonons, surface roughness, and optical phonons as well as for scattering by combined acoustic phonons and surface charges. The current-voltage characteristic is also calculated for high electric fields using a Maxwellian distribution with electron temperature T_e. These results are compared with experimental values obtained in this paper and those given by Fang and Fowler.

I. INTRODUCTION

This paper concerns the motion of electrons in silicon inversion layers in strong electric fields parallel to the surface. A n-type inversion layer is produced at the surface of a p-type semiconductor when the energy bands near the surface are bent down enough, so that the bottom of the conduction band lies near the Fermi level. We assume that the electric field associated with the inversion layer is strong enough to produce a potential well whose width in the direction perpendicular to the surface is small compared to the electron wavelength. Thus the energy levels of the electrons are grouped into subbands.

The case when only the lowest subband is populated is called the electrical quantum limit. There exists strong experimental and theoretical evidence that the charge carriers behave as a two-dimensional gas in such a surface-inversion channel.[1,2] The energy difference between the first subbands is of the order of 10–100 meV. From this one can see that even if more than one subband is populated, the motion and scattering of the carriers perpendicular to the surface must be considerably impeded, since the phonon energies are smaller than 100 meV. Most of the perpendicular transitions are, therefore, forbidden.

As a consequence of the two-dimensional structure, the density of states in the different subbands does not depend on energy ϵ, as $dk_x dk_y$ is simply proportional to $d\epsilon$. This causes drastic changes in the scattering processes, since the scattering probability is proportional to the density of final states. The scattering probability, e.g., for scattering by acoustical phonons, becomes independent of energy, whereas in the three-dimensional case it is proportional to $\epsilon^{1/2}$.

The high-field behavior of bulk semiconductors has been investigated in considerable detail. A comprehensive analysis was given by Conwell.[3] It turned out that the assumption of a carrier temperature T_e larger than the lattice temperature gives a useful semiquantitative description of the high-field transport phenomena. It was pointed out,[4,5] however, that this concept breaks down if inelastic scattering dominates. One of the main reasons for the breakdown is that the number of carriers n_0 above the optical-phonon energy $\hbar\omega_R$ is overestimated. This leads to large errors in the calculation of the mean energy loss, which depends strongly on n_0, as only the carriers above $\hbar\omega_R$ can emit optical phonons. Criteria have been given in the literature[6] for the validity of the electron-temperature concept. All of them, however, are rather crude.

We will show, by solving the Boltzmann equation in the diffusion approximation for a two-dimensional carrier gas, that the use of the electron temperature concept is better justified as compared to the three-dimensional case.

In Sec. II we establish the Boltzmann equation. The collision operators are given for scattering by acoustical as well as nonpolar optical phonons. In Sec. III we give approximate solutions of the Boltzmann equation for the warm-carrier region and in Sec. IV for the region of very high electric fields. These solutions are compared with the approximation using the electron-temperature concept. In Sec. V experimental results for the warm electron region are presented. Our samples were n-channel Si-field-effect transistors with (110) surface and ⟨100⟩ and ⟨110⟩ channel orientation.

Finally in Sec. VI a comparison between the theory and experimental result is given.

II. TWO-DIMENSIONAL BOLTZMANN EQUATION

As mentioned, Conwell[3] gave a comprehensive analysis of the formulation of the Boltzmann equation for the three-dimensional case. Since all the calculations proceed very similarly for the two-

dimensional case considered here, we give only a brief description of the main new features.

The structure of the subbands has been given by Stern.[1] The lines of constant energy are ellipses which arise from the intersection of the ellipsoids with the surface plane. We will give the magnitude of the axes of the ellipses whenever a comparison with experimental results is made. In this section, however, we will write down the equations in the starred system of coordinates for the ith ellipse in which the ith ellipse is a circle. In the interest of less cumbersome notation we do not mark the quantities of the starred system separately, except where this would lead to ambiguity. In this case, we mark the quantities of the starred system by an asterisk.

As in the three-dimensional case a relaxation time exists in the low-field region since the two-dimensional optical matrix element does not depend on the wave vector $\vec{k}$ of the electrons. Because of the lack of a better theory we assume the scattering to be isotropic. Furthermore it is assumed that the momentum randomization is mainly governed by elastic scattering processes. This assumption seems to be quite reasonable, as in most of the experiments of strongly inverted surface, surface-roughness scattering[7,8] plays an important role. With this in mind we write for the distribution function f:

$$f = f_0(\epsilon) + k_E g_e(\epsilon)\,, \tag{1}$$

where $f_0(\epsilon)$ is spherical part of f, $g_e(\epsilon)$ is the drift term, k_E is the component of $\vec{k}$ in the direction of the electric field $\vec{E}$, and ϵ is the carrier energy. Writing the Boltzmann equation symbolically:

$$\left(\frac{\partial f}{\partial t}\right)_E + \left(\frac{\partial f}{\partial t}\right)_c = 0\,, \tag{2}$$

we obtain for the field term

$$\left(\frac{\partial f}{\partial t}\right)_E = -\frac{eE}{\hbar}\left(\frac{\hbar^2 k_E}{m}\frac{df_0}{d\epsilon} + g_e + \epsilon\frac{dg_e}{d\epsilon}\right) \tag{3}$$

after replacing $\hbar^2 k_E^2/m$ by its two-dimensional average value.

Inserting for

$$\left.\frac{\partial(k_E g_e)}{\partial t}\right|_c = -k_E g_e/\tau_k\,, \tag{4}$$

one obtains from Eq. (2)

$$\left(\frac{\partial f_0}{\partial t}\right)_c - \frac{eE}{\hbar}\left(g_e + \epsilon\frac{dg_e}{d\epsilon}\right) = 0 \tag{5}$$

and

$$g_e = -\frac{e\hbar E\tau_k}{m}\frac{df_0}{d\epsilon}\,, \tag{6}$$

where τ_k is the momentum relaxation time, where for simplicity k is dropped in later use.

Now we need to calculate the collision operator $(\partial f_0/\partial t)_c$ for scattering by acoustical and optical phonons. The collision operator is written as usual:

$$\left(\frac{\partial f_0}{\partial t}\right)_c = -\int [f_0(\vec{k})P(\vec{k}\to\vec{k}') - f_0(\vec{k}')P(\vec{k}'\to\vec{k})]d^2k'\,. \tag{7}$$

$P(\vec{k}\to\vec{k}')\,d^2k'$ represents the probability per unit time that a carrier with $\vec{k}$ is scattered into the element of area d^2k' at $\vec{k}'$.

The square of the matrix element for scattering by acoustic phonons is written

$$|\langle\vec{k}|H_{ac}|\vec{k}\pm\vec{q}\rangle|^2 = (Z_A^2\hbar\omega_q/2\rho A u_l^2)(N_q + \tfrac{1}{2} \mp \tfrac{1}{2})\delta_{\vec{k}',\vec{k}\pm\vec{q}}\,, \tag{8}$$

where $\hbar\omega_q$ is the energy of a phonon with wave vector $\vec{q}$, N_q is the phonon occupation number, u_l is the longitudinal sound velocity, A is the surface area, and Z_A is the acoustical surface deformation potential in eV. ρ has the dimension of an areal mass density. Detailed analyses have been given by Kawaji and Ezawa *et al.* which show the physical significance of ρ and Z_A. The papers of Kawaji and Ezawa *et al.* are referenced in footnote 9 and denoted by K1 and K2 as well as E1 and E2 in the following. Based on a two-dimensional lattice model it is shown in K1 that $\rho = \rho_{(3\text{-dim})} \times d$. Subsequently Kawaji (K2) refined his calculations to show that $\rho = \rho_{(3\text{-dim})} \times d \times \frac{16}{9}$. Here $d = 3/b$ and b is defined by the Howard wave function $z\, e^{(-bz)}$ as employed by Stern and Howard.[1]

It was concluded, however, in E1 and E2, that the interaction of the channel electrons with "surfons" (the quanta of Reileigh waves) is weaker as compared to the interaction of the electrons with ordinary bulk phonons. This conclusion is based on an "accidental" cancellation of tensor components of the deformation-potential constant, which appears in the matrix element for "surfonscattering."

We should like to note, that deformation-potential constants as given, e.g., in our Refs. 15 and 20 would not lead to the result of E1, though surfons would still be less important.

The fact that scattering by bulk phonons dominates does *not* mean, of course, that scattering in z direction is important for the mobility. Howard's wave function was used in E2 to calculate the form factor of the matrix element. As shown above this wave function decays exponentially in z direction (typically $b \sim 3\times10^6$ cm^{-1}) and makes the transition probability in z direction very small.

The formulas for the transition probability and the momentum relaxation time which are given in E2 are equivalent to our Eq. (8) and the following Eq. (13) and to the equations given in K1 and K2 except for the interpretation of the constants de-

noted by ρ and Z_A in our paper. We determined Z_A and ρ by fitting the experimental values of the mobility as was done previously,[2] since we feel that this phenomenological procedure will provide the best results at the present status of the theory.

The matrix element for optical or intervalley phonons is given by[2]

$$|\langle\vec{k}|H_{\rm opt}|\vec{k}\pm\vec{q}\rangle|^2=(Z_R^2\hbar\omega_R/2\rho A u_l^2)(N_R+\tfrac{1}{2}\mp\tfrac{1}{2})\delta_{\vec{k}',\vec{k}\pm\vec{q}}\ . \tag{9}$$

The various quantities are indexed now with R to distinguish them from the corresponding acoustic quantities. Inserting Eq. (8) into Eq. (7) we obtain in cylinder coordinates

$$\left(\frac{\partial f_0}{\partial t}\right)_{\rm ac}=M\int dq\,d\phi\,\{q\delta(q+q_\alpha)[f_0(\vec{k}+\vec{q})(N_q+1)-f_0(\vec{k})N_q] + q\delta(q-q_\alpha)[f_0(\vec{k}-\vec{q})N_q-f_0(\vec{k})(N_q+1)]\}. \tag{10}$$

Here $q_\alpha=2k\cos\phi-2mu_l/\hbar$ and $M=Z_A^2 m_l m_t/2\pi m\hbar^2\rho u_l$. Integrating first over q and then over ϕ one obtains:

$$\left(\frac{\partial f_0}{\partial t}\right)_{\rm ac}=(2m_lm_tZ_A^2/\hbar^3\rho)\frac{d}{dx}\left[x\left(\frac{df_0}{dx}+f_0\right)\right] =S_A\frac{d}{dx}\left[x\left(\frac{df_0}{dx}+f_0\right)\right], \tag{11}$$

where $x=\epsilon/k_BT$, $f_0=f_0(x)$, and $S_A=2m_lm_tZ_A^2/\hbar^3\rho$.

We also find the collision operator for optical modes by inserting Eq. (9) in Eq. (7):

$$\left(\frac{\partial f_0}{\partial t}\right)_{\rm opt}=\sum_R S_R\{(N_R+1)f_0(x+x_R)-N_Rf_0(x) +\Theta(x-x_R)[N_Rf_0(x-x_R)-(N_R+1)f_0(x)]\}, \tag{12}$$

where Θ is the step function, $x_R=\hbar\omega_R/k_BT$, and

$$S_R=(m_lm_t)^{1/2}Z_R^2\hbar\omega_R/2\hbar^3\rho u_l^2 .$$

Next we need to know the momentum relaxation times τ for calculating the field term which are given below. The relaxation time due to scattering by acoustic phonons does not depend on energy. It is given by[2]

$$1/\tau_{\rm ac}=(m_lm_t)^{1/2}Z_A^2k_BT/\hbar^3\rho u_l^2 . \tag{13}$$

The relaxation time for scattering by surface roughness[7,8] is also independent of energy. We can therefore combine it with $\tau_{\rm ac}$ for many purposes. We denote the scattering by surface roughness by τ_r and the combined relaxation time by $\tau_{{\rm ac}\,r}$.

The relaxation time for optical-phonon scattering is[2]

$$1/\tau_{\rm opt}=\sum_R[(m_lm_t)^{1/2}Z_R^2\hbar\omega_R/2\hbar^3\rho u_l^2] \times[(N_R+1)\Theta(x-x_R)+N_R]. \tag{14}$$

For n-silicon R runs only over intervalley processes. The relaxation time τ_I for scattering by surface ions is more complicated.[10] From the analogy to the three-dimensional case one can expect a strong anisotropy. Furthermore, it depends on a number of quantities, e.g., the spatial distribution of the electrons and the ions in the interface region, ion position correlation, and electron screening. In order to simplify the calculation we write

$$1/\tau_I=\epsilon'/\epsilon . \tag{15}$$

Here ϵ' is only weakly dependent on ϵ and it is assumed to be a constant to be extracted from the experiments using

$$1/\tau=1/\tau_{\rm ac}+1/\tau_{\rm opt}+1/\tau_I+1/\tau_r . \tag{16}$$

The value of ϵ' is given in Ref. 10.

One can now formulate the equation for the spherical symmetrical part f_0 of the distribution function f by combining Eqs. (5), (6), (11), (12), and (16):

$$\sum_R S_R\{(N_R+1)f_0(x+x_R)-N_Rf_0(x)+\Theta(x-x_0) \times[N_Rf_0(x-x_R)-(N_R+1)f_0(x)]\} +S_A\frac{d}{dx}\left[x\left(\frac{df_0}{dx}+f_0\right)\right] =-\frac{e^2E^2\tau}{mk_BT}\frac{d}{dx}\left[x\left(\frac{df_0}{dx}\right)\right] . \tag{17}$$

Note that electron-electron scattering has not been included in Eq. (17) since explicit results cannot be obtained. Its effects will be discussed briefly in the next section.

If we confine our calculations to the case where the subband under consideration contains only identical valleys (valleys with parallel main axes) Eq. (17) has to be solved subject to the following boundary conditions:

$$\frac{2}{(2\pi)^2}\int_{-\infty}^{+\infty}f_0(x)\,dk_x\,dk_y=n . \tag{18}$$

Here n is the number of electrons in the valley under consideration, and

$$\lim_{x\to\infty}x^\alpha f_0(x)=0 \text{ for } \alpha>0. \tag{19}$$

As pointed out by Adawi,[11] (19) is necessary for the moments of the distribution to be finite.

III. SOLUTIONS FOR SMALL E—WARM ELECTRONS

For small electric fields E we write

$$f_0(x)=A[1+(E/E_0)^2\xi(x)]e^{-x}, \tag{20}$$

with $\int_0^\infty e^{-x}\xi(x)\,dx=0$ to fulfill Eq. (18). We now solve Eq. (17) for three different cases. In all cases under consideration Eq. (19) means that the

first integration constant, which appears by solving Eq. (17) is zero.

1. Acoustical phonons surface roughness

If the electrons are scattered by acoustical phonons and surface roughness only, and E is weak enough so that all powers of E except the second can be neglected, Eq. (17) reads:

$$\frac{d}{dx}\left[xe^{-x}\left(\frac{d\xi}{dx}\right)\right]=\frac{d}{dx}(xe^{-x}), \tag{21}$$

with $E_0^2=S_A mk_BT/e^2\tau_{\mathrm{ac}\,r}$ and $\tau_{\mathrm{ac}\,r}^{-1}=\tau_{\mathrm{ac}}^{-1}+\tau_r^{-1}$.

The solution of (21) is:

$$\xi(x)=x-1. \tag{22}$$

This solution is equivalent to the first-order expansion of a Maxwellian distribution function with electron temperature T_E since

$$e^{-\epsilon/k_BT_e}=e^{-\epsilon/k_B(T_e-T+T)}\simeq e^{-x}/[1+x(T_e-T)/T]$$

for small $(T_e-T)/T$. Note that the analogous three-dimensional solution is not Maxwellian, which is[11]

$$\xi(x)=\ln x-\int_0^\infty x^{1/2}e^{-x}\ln x\,dx=\ln x-0.032\,34.$$

2. Acoustical phonons and surface ions

At very low temperatures optical phonons are unimportant and $\tau\simeq\tau_I$. Equation (17) can then be written

$$\frac{d}{dx}\left[xe^{-x}\left(\frac{d\xi}{dx}\right)\right]=x\frac{d}{dx}(xe^{-x}), \tag{23}$$

with $E_0^2=mS_A\epsilon'/e^2$.

The solution of Eq. (23) is

$$\xi(x)=\tfrac{1}{2}x^2+x+\ln x+K_1. \tag{24}$$

The constant K_1 has to be determined from the boundary conditions. Care must be taken for small x where $\ln x$ becomes negative. To avoid negative f_0, we have to require that f_0 is zero below a certain x value denoted by x_d. Equation (20) gives for x_d

$$(\tfrac{1}{2}x_d^2+x_d+\ln x_d+K_1)(E/E_0)^2=-1.$$

For small x_d values this reduces to

$$x_d=\exp\{-[(1+K_1(E/E_0)^2)/(E/E_0)^2]\}.$$

K_1 can be obtained from the normalization condition. For small x_d it can be approximated by $K_1\simeq\gamma-2$. $\gamma=0.577\,215\,7$ is Eulers constant. Thus the distribution function shows a "low-energy depletion." One can understand this from the fact that the probability of a carrier being scattered decreases with increasing energy, when impurity scattering dominates. Thus electrons with high energy gain more energy from the field than the slow electrons and the distribution function is shifted to higher energies. The inclusion of optical phonons causes the reversed effect a "high-energy depletion" as we will see in the next section.

3. Acoustical and optical phonons

In this case the calculations are complicated because of the cumbersome terms $f(x\pm x_0)$, which arise from the convolution in Eq. (7). If we confine ourselves to one optical phonon mode only and insert Eq. (20) into Eq. (17) we obtain

$$\frac{d}{dx}\left[xe^{-x}\left(\frac{d\xi}{dx}\right)\right]+(S_R/S_A)N_Re^{-x}\{[\xi(x+x_R)-\xi(x)]+\Theta(x-x_R)e^{x_R}[\xi(x-x_R)-\xi(x)]\}=g(x)\frac{d}{dx}(xe^{-x}), \tag{25}$$

with $E_0^2=S_Amk_BT/e^2\tau_{\mathrm{ac}\,r}$ and $g(x)=\tau_{\mathrm{opt}}/(\tau_{\mathrm{opt}}+\tau_{\mathrm{ac}\,r})$.

An equation similar to Eq. (25) arises in the three-dimensional case. Variational methods have been used to solve it.[11] In our case, however, we can obtain an explicit solution for large values of x_R. For large x_R, N_R is very small and the absorption term in Eq. (25) can be entirely neglected.[12] The emission term however is proportional to e^{x_R} and is therefore large even for very low temperatures. $g(x)$ is a step function as can be seen from Eqs. (13) and (14). We will denote it by $g_<$ and $g_>$ for $x\le x_R$ and for $x>x_R$, respectively. Thus for $0<x\le x_R$ we have

$$\frac{d}{dx}\left[xe^{-x}\left(\frac{d\xi}{dx}\right)\right]=g_<\frac{d}{dx}(xe^{-x}) \tag{26}$$

and the solution is

$$\xi(x)=a_1x+b_1, \tag{27}$$

where $a_1=g_<$ and b_1 is given below.

For $x_R<x\le 2x_R$ Eq. (25) reads

$$\frac{d}{dx}\left[xe^{-x}\left(\frac{d\xi}{dx}\right)\right]+(S_R/S_A)N_Re^{-x}e^{x_R}[a_1(x-x_R)-b_1-\xi(x)]=g_>\frac{d}{dx}(xe^{-x}). \tag{28}$$

Since $\xi(x-x_R)$ belongs (for the above given range of x values) to solutions of (26) and is therefore given by $a_1(x-x_R)-b_1$.

As can be found by inspection the solution of Eq. (28) is again a polynominal of first order

$$\xi(x)=a_2x+b_2. \tag{29}$$

The process can be easily continued for $2x_R<x\le 3x_R$, etc. For all practical purposes however the knowledge of the distribution function above $2x_R$ is not necessary because of the strongly decreasing exponent. Remember that the whole solution is only valid for large x_R.

Inserting Eq. (29) into Eq. (28) we find for a_2

and b_2,

$$a_2 = (g_> + s g_<)/(1+s)\,, \tag{30}$$

$$b_2 = [a_2 - g_> - s(g_< x_R - b_1)]/s\,, \tag{31}$$

where $s = (S_R/S_A) N_R e^{x_R}$ and b_1 is obtained from the normalization condition

$$-b_1 = g_< \gamma(2, x_R) + a_2[1 - \gamma(2, x_R)] + [(a_2 - g_> - s x_R g_<)/s] e^{-x_R}. \tag{32}$$

Here

$$\gamma(2, x_R) = \int_0^{x_R} x e^{-x}\, dx$$

is the incomplete γ function.

A distribution function according to Eqs. (27) and (30)–(32) is shown in Fig. 1. The parameters used are listed in Table I, set 1. The effective masses are calculated for the lowest subband of a (110) silicon surface and $E = 500$ V/cm in ⟨110⟩ direction. Note the distinct kink at x_R in Fig. 1 which indicates that the number of carriers above x_R is strongly reduced by the optical phonons as compared to a Maxwellian distribution at electron temperature T_e as indicated by the dotted line. Although this depletion of electrons occurs at high-x values where the number of electrons is small, it can be important for various transport phenomena as we will show below.

4. Transport quantities

One of the most important quantities for the description of hot-electron phenomena is the mean energy loss per carrier to the lattice $\langle d\epsilon/dt\rangle$ given in two dimensions by

$$\left\langle \frac{d\epsilon}{dt} \right\rangle = \frac{1}{n} \frac{2}{(2\pi)^3} \int_{-\infty}^{+\infty} \frac{\partial f_0}{\partial t}\bigg|_c \epsilon\, dk_x\, dk_y\,. \tag{33}$$

In some cases $\langle d\epsilon/dt\rangle$ depends strongly on the number of carriers n_0 above x_R, since only these carriers can emit optical phonons. The warm-electron coefficient defined by $\mu = \mu_0(1+\beta E^2)$ is closely related to the energy loss. To show this we define as usual an energy relaxation time τ_ϵ by the equation

$$\Delta/\tau_\epsilon = \left\langle \frac{d\epsilon}{dt} \right\rangle,$$

where Δ is the mean energy deviation from $k_B T$ of the carriers: $\Delta = \langle \epsilon - k_B T\rangle$. In the stationary state the power dissipation to the lattice equals to the power supplied by the field

$$\left\langle \frac{d\epsilon}{dt} \right\rangle = e\mu E^2 \simeq e\mu_0 E^2\,.$$

Expanding now μ in terms of Δ: $\mu = \mu_0 + (d\mu/d\Delta)\Delta$ one obtains for β:

$$\beta = \left(\frac{d\mu}{d\Delta}\right) \tau_\epsilon e\,. \tag{34}$$

As one can see from the definition, τ_ϵ is a constant as long as the expansion of Eq. (20) holds. The expansion of μ in terms of Δ however is rather crude and holds only for a limited class of distribution functions. The Maxwellian with an electron temperature T_e belongs to this class.

Let us consider now how scattering by optical phonons acts on β. To do this we assume first that the term $d\mu/d\Delta$ does not depend on the optical coupling constant Z_R. The whole dependence of β on Z_R is then contained in τ_ϵ. Let us further assume that β is known from experiments and Z_R is extracted from the experimental value of β. Now we distinguish two cases:

(i) Z_R is large, but we do not know this. Then if we believe that the distribution function is Maxwellian with electron temperature T_e, we would overestimate the energy loss, as we overestimate the number of carriers above x_R. It follows that the values of τ_ϵ and β calculated using the Maxwellian distribution with T_e with the correct Z_R would be much too small. To fit the β value, we must use a value of Z_R which is much smaller than it really is. This conclusion is self-consistent as the distribution function tends to a Maxwellian when Z_R is small.

(ii) Z_R is small, but we do not know this. Then if we believe now that the distribution function is of the type shown in Fig. 1, we would underestimate the number of carriers above x_R as long as Z_R is truly small. Thus we have to choose a fairly high value of Z_R in order to fit the experiment. Again our conclusion is self-consistent, as the distribution function has the form shown in Fig. 1 for high Z_R. As a numerical example, if one fits a value of $\tau_\epsilon = 1.4\times10^{-11}$ sec for $T = 150$ °K, $\Theta = 670$ °K and the masses of Table I one obtains: (1) $b = 5.3$ using a distribution function from Eqs. (27), (30),

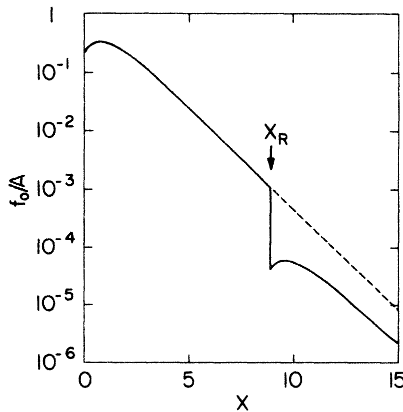

FIG. 1. Spherical part of the distribution function for acoustical plus optical plus surface-roughness scattering.

TABLE I. Constants used in the calculations.

Set 1 for $T=77\,^\circ\mathrm{K}$					
Z_A	Z_1	$\tau_{ac\,r}$	Θ_1	m_l	m_t
7.65 eV	17.6 eV	6×10^{-13} sec	670 K	$0.55m$	$0.19m$
Set 2 for $T=77\,^\circ\mathrm{K}$ (Z_A, m_l, m_t same as set 1)					
Z_1	Z_2	$\tau_{ac\,r}$		Θ_1	Θ_2
17.6 eV	7.4 eV	7.4×10^{-13}sec		670 K	190 K

and (31); (2) $b=1.7$ using a Maxwellian at T_e. Here $b=(Z_R/Z_A)^2$. Z_A is given in Table I. The agreement becomes better however if $d\mu/d\Delta$ also depends on the optical coupling constant.

Distribution functions as shown in Fig. 1 arise also in the hot-electron region of the three-dimensional case, as obtained from various numerical methods.[5,12–14] The number of electrons above x_R is reduced by optical scattering also in these cases. The optical phonon emission seems to "overkill" itself quite generally. In Appendix A we will show that the simple method for calculating f_0 used in this paper can partly be applied to the three-dimensional case and yields qualitatively the same results as those for two dimensions.

So far we did not consider electron-electron scattering. The inclusion of e-e scattering would make explicit results impossible. It is also clear that distribution functions like that of Fig. 1 cannot be described well by a variational method, since the approximation of $\xi(x)$ with one single polynomial would require a large number of terms. In the three-dimensional case, e-e scattering shifts the distribution function to the Maxwellian type.[6] One can expect that it has the same effect in two dimensions.

Using the distribution function $Ae^{-x}[1+(E^*/E_0)^2\times\xi(x)]$ and calculating the current j from

$$j=-\frac{e^2}{m}E^*_{l,t}\int_0^\infty\frac{df_0}{dx}\tau_m\epsilon\,d\epsilon,$$

we obtain for the two-dimensional β,

$$\beta_{l,t}=\frac{1}{\mu_{l,t}}\frac{eE^{*2}_{l,t}}{mE_0^2E^2}\int_0^\infty\tau_m xe^{-x}\left[\xi(x)-\frac{d\xi(x)}{dx}\right]dx\,. \tag{35}$$

Here we have assumed that $\vec{E}$ points in the direction of one of the main axis (l,t) of the ellipsoid.

We did not find a solution for $\xi(x)$, for the case that all mentioned scattering mechanisms are important simultaneously. However, we can find a value for β using the Maxwellian approach and Eq. (34) including now all scattering mechanisms. In order to get explicit results we take into account only one type of optical phonons and assume $\tau_I\gg\tau_{ac\,r}$.

Combining Eqs. (13)–(16) and (34) and taking the two-dimensional average for calculating $\langle\epsilon\tau\rangle/\langle\epsilon\rangle$, we obtain

$$\beta_{l,t}=((\mu_{ac}/\mu_I)\{(1-e^{-x_R})(1+\tau_{ac}S_RN_R)^{-2}+e^{-x_R}[1+\tau_{ac}S_R(2N_R+1)]^{-2}\}+x_R^2e^{-x_R}[(1+\tau_{ac}S_RN_R)^{-1}-[1+\tau_{ac}S_R(2N_R+1)]^{-1}])(\mu/\mu_{ac})(\Delta_{l,t}/E^2T)\,, \tag{36}$$

where $\Delta=\langle\epsilon-k_BT\rangle$ and μ_1 the mobility due to scattering by ionized impurities. μ is the mobility due to all scattering mechanisms involved.

From Eqs. (33) and (11) we obtain for the energy loss due to scattering by acoustic phonons

$$\left\langle\frac{d\epsilon}{dt}\right\rangle_{ac}=(2m_lm_tZ_A^2/\hbar^3\rho)(k_BT-k_BT_e)\,. \tag{37}$$

The combination of Eqs. (33) and (12) gives for the loss to optical phonons

$$\left\langle\frac{d\epsilon}{dt}\right\rangle_{opt}=[(m_lm_t)^{1/2}Z_R^2\hbar^2\omega_R^2/2\hbar^3\rho u_l^2]\times[N_R+(N_R+1)\exp(-x_R^e)]\,, \tag{38}$$

here $x_R^e=\hbar\omega_R/k_BT_e$.

For $k_BT_e-k_BT_e\equiv\Delta\ll k_BT$ one can expand $\exp(-x_R^e)$ in terms of Δ which gives $e^{-x_R}(1+x_R\Delta/T)$. Equations (37) and (38) are then linear in Δ and $\Delta_{l,t}$ can be calculated from the relation

$$e\mu_{l,t}E^2=\left\langle\frac{d\epsilon}{dt}\right\rangle=\left\langle\frac{d\epsilon}{dt}\right\rangle_{ac}+\left\langle\frac{d\epsilon}{dt}\right\rangle_{opt}.$$

Figure 2 shows β values calculated for set 1 of material constants of Table I. The upper curve (I) is calculated with the distribution function given in Sec. III 3, the lower (II) with a Maxwellian at T_e. The increase of β with temperature at low temperature arises from the fact that $\tau_{ac\,r}$ is independent

of energy and the deviations from Ohms law are governed only by optical scattering which becomes stronger at higher temperature. At still higher temperatures, however, the optical energy loss becomes very strong and β decreases.

IV. HOT ELECTRONS

In the preceeding section we analyzed the warm-electron cases. In this section, the characteristics of the solutions of the Boltzmann's equation for the hot-electron–high-field range are studied in the various sections given below.

1. Acoustical phonons and surface roughness

For only acoustical phonon and surface roughness scattering in strong electric fields Eq. (17) reads:

$$S_A \frac{d}{dx}\left[x\left(\frac{df_0}{dx}+f_0\right)\right] = -\frac{e^2E^{*2}\tau_{ac\,r}}{mk_B T}\frac{d}{dx}\left(x\frac{df_0}{dx}\right) \quad (39)$$

The solution is

$$f_0 = A\exp[-x/(1+E^{*2}/E_0^2)], \quad (40)$$

where $E_0^2 = mk_BTS_A/e^2\tau_{ac\,r}$ and A is a normalization constant. This means that f_0 is a Maxwellian distribution with electron temperature $T_e = T(1+E^{*2}/E_0^2)$

Since for many experimental conditions $\tau_{ac\,r}$ is important we can conclude that a Maxwellian distribution will be a better approximation for the two-dimensional case than the three-dimensional case, as in three dimensions the distribution function is not Maxwellian even for acoustical scattering alone.

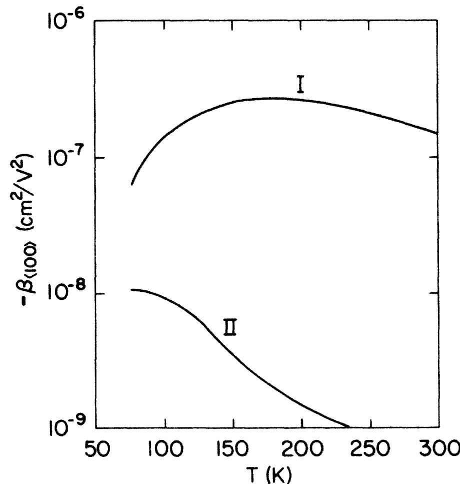

FIG. 2. Warm-electron coefficient β for E in $\langle$ 10$\rangle$ direction using a non-Maxwellian (I) and a Maxwellian (II) distribution function and the same set of material constants.

2. Combined acoustical and optical phonons and surface roughness

At very high electric fields the mean energy of the electrons becomes much larger than the optical-phonon energy. One can then make the following expansion:

$$f_0(x \pm x_R) = f_0(x) \pm x_R\left(\frac{df_0}{dx}\right).$$

After one integration, Eq. (17) reads

$$\frac{1}{f_0}\frac{df_0}{dx} = -\frac{S_Ax+S_Rx_R}{x(S_A - S_{AR}g_>)}, \quad (41)$$

the solution of Eq. (41) is

$$f_0 = A\,e^{-S_Rx_R/(S_A-S_{AR}g_>)}\,e^{-S_Ax/(S_R-S_{AR}g_>)} \quad (42)$$

Here $S_{AR} = -e^2E^{*2}\tau_{ac\,r}/mk_BT$ and A is a constant.

A distribution function derived in a similar way for the three-dimensional case was given in Conwell.[3] f_0 from Eq. (42) is very nearly Maxwellian with T_e for not too large a S_R in contrast to the corresponding three-dimensional distribution function. Equation (42) seems, however, to have no practical interest. In the range of its validity all subbands are populated due to high electric fields and the scattering cannot be regarded as two dimensional.

3. Current-voltage characteristic for a Maxwellian-type distribution function

With the assumption of v equivalent valleys in the lowest subband and isotropic scattering, the current equation in α direction for the ith valley is

$$j_\alpha^i = n^i\mu_\alpha^{i*}E_\alpha^{i*}. \quad (43)$$

Here we allow the number of electrons n^i in the ith valley to be different for different i. Whereas in Sec. III 4 a repopulation of carriers was not considered.

The reason for this specialization will become clear in Sec. VI, where the arrangement of the valleys in the different subbands will be discussed.

The electron temperature in each valley can now be derived from the steady-state power balance condition

$$e\vec{E}^*\cdot\mu^{i*}(T_e^i)\vec{E}^* = \left\langle\frac{d\epsilon}{dt}\right\rangle^i. \quad (44)$$

The particle number in the different valleys can be calculated from

$$\sum_m{}'\left(\frac{\partial n}{\partial t}\right)_{m\to i} = \sum_j{}'\left(\frac{\partial n}{\partial t}\right)_{i\to j}. \quad (45)$$

Where $\sum_j'$ means the sum over all valleys except the ith. $(\partial n/\partial t)_{i\to j}$ is the transfer rate of carriers from valley i to valley j given by[3]

$$\left(\frac{\partial n}{\partial t}\right)_{i\to j} = -\langle 1/\tau_{opt}^{i\to j}\rangle n^i. \quad (46)$$

This gives

$$n^i = n\left(f^i \sum_l \frac{1}{f^l}\right) \tag{47}$$

where

$$f^i = \sum_R [N_R + (N_R+1)\exp(\hbar\omega_R/k_B T_e^i)]\hbar\omega_R Z_R^2 \, .$$

The calculation proceeds now as usual: (i) calculate T_e^i from Eq. (44) with help of Eqs. (37) and (38); (ii) calculate n^i from Eq. (47); (iii) calculate the current from Eq. (43).

V. EXPERIMENTAL RESULTS

We performed experiments at 77 °K. The samples used were typical n-channel field-effect metal-oxide-semiconductor (MOS) transistors, with 0.002-in. channel length and an oxide thickness of 5000 Å. The devices are made on a (110) p-Si surface with an acceptor concentration $N_A = 2.2 \times 10^{14}/\text{cm}^3$. The channel was oriented in ⟨100⟩ and ⟨110⟩ direction. The devices with different channel orientations were processed in two device fabrication runs: (i) on separate wafers with both wafers being processed simultaneously and (ii) on the same wafer. These devices were fabricated by Edwards[16] and some results on orientation dependence of low-temperature (4.2 °K) and low-field mobility[17] were reported.

The samples with the same channel orientation, obtained from both device runs show nearly identical conductivity. The mobility versus gate voltage of samples with ⟨100⟩ and ⟨110⟩ channels was extremely uniform. For nearly flat band condition the 77 °K conductivity mobility was: $\mu^{\langle 110\rangle}_{\langle 100\rangle} = 4000$ cm^2/V sec, $\mu^{\langle 110\rangle}_{\langle 110\rangle} = 2800$ cm^2/V sec. For high gate voltages, when the number of the inverted carriers is about $3\times 10^{12}/\text{cm}^2$ typical values are: $\mu^{\langle 110\rangle}_{\langle 100\rangle} = 2350$ cm^2/V sec and $\mu^{\langle 110\rangle}_{\langle 110\rangle} = 1900$ cm^2/ V sec at 77 °K. The number of surface state charges Q_{SS} of these samples has been measured with various methods.[16] Q_{SS} is less than about $5\times 10^{10}/\text{cm}^2$.

The source-drain conductance at high fields was measured using a standard pulsed bridge technique. Source drain formed one arm of the Wheatstone bridge. A dc bias was applied to the gate for inverting the surface. For balancing the bridge an oscilloscope with differential plug-in was used. The pulse width was typically 800 nsec. Measuring points have been taken after 400 nsec. No time dependence of the pulse could be observed from 100–800 nsec.

Since the drain depletion with increasing drain voltage could cause a considerable amount of the deviations of Ohm's law in these devices we used the following method of evaluation.

For small deviations from Ohm's law due to warm-carrier effects, the equation for the drain current can be written as[18]

$$I_D = (Z/L)\,\mu_0 C_0 (1+\beta E^2)\{(V_G - \psi_{S0} - \phi_{ms} + Q_{SS}/C_0)V_D - \tfrac{1}{2}V_D^2 - (\tfrac{4}{3}\phi_F V_B)[(1+V_D/2\phi_F)^{3/2} - 1]\}$$
$$+ (Z/L)\, C_0 \frac{d\mu_0}{dV_G} V_D^2 (V_G - \psi_{S0} - \phi_{ms} + Q_{SS}/C_0)/2 \, . \tag{48}$$

Here V_D is the drain voltage, $V_B = (4qN_A K_S \epsilon_0 \phi_F / C_0)^{1/2}$, K_S is the dielectric constant of the semiconductor, C_0 is the oxide capacity per unit area, ϕ_F is the Fermi potential in the bulk, and ψ_{S0} is the surface potential for zero drain to source bias. The last term arises mainly because of the dependence of all the scattering mechanisms on the mean distance of the electrons from the surface.[8,19]

For our devices all nonlinear terms in V_D are estimated to be smaller than about $\frac{1}{3}$ of βE^2 in the range of fields E and gate voltages investigated. However, we eliminated the effect from other nonlinear terms by the following procedure. If one measures at two different gate voltages, a and b, with constant drain voltage one obtains from Eq. (48)

$$\left(\frac{R_0^a}{R^a} - 1\right) V_G^a{*} - \left(\frac{R_0^b}{R^b} - 1\right) V_G^b{*} - \frac{1}{2}\frac{d\ln\mu_0^a}{d\ln V_G^a} V_D + \frac{1}{2}\frac{d\ln\mu_0^b}{d\ln V_G^b} V_D = \beta(V_G^a{*} - V_G^b{*})(V_D/L)^2 . \tag{49}$$

Here R_0 is the resistance of the channel at $V_D = 0$ and R is the resistance at V_D. $V_G{*} = V_G - \psi_{S0} - \phi_{ms} + Q_{SS}/C_0$. The indices a or b indicate that the values are taken at gate voltages a or b. To obtain Eq. (49) from Eq. (48) we have neglected V_B compared with V_G. Furthermore, we assumed that $V_G{*} - V_G$ is independent of the gate voltage, which is a quite reasonable assumption for the low surface-state density of our devices and the high gate voltages used, as the threshold voltage was about 0.3 V and the gate voltages used are in the range of 25–100 V.

The value of the terms proportional to $d\mu/dV_G$ have been evaluated from measurements at low fields, where the right-hand side of Eq. (49) is essentially zero.

The tacit assumption of Eq. (49) is that β does

not change with the gate voltage. Measurements at more than two different gate voltages show that β decreases approximately proportional to the mobility decrease as the gate voltage increases. This is plausible also from the theory since β is proportional to Δ which is proportional to the mobility. This effect gives an additional correction (about 20% at our experimental conditions) to β. To obtain the correct value of β^b at the gate voltage V_G^b one has to replace the right-hand side of Eq. (49) by

$$\beta^b(V_D/L)^2[V_G^a{}^* - (\mu_0^b/\mu_0^a)\, V_G^b{}^*] . \tag{50}$$

Figure 3 shows $1 - R_0/R$ measured at two different gate voltages vs the drain voltage. The channel orientation was ⟨100⟩. The measuring points have been obtained from four different devices. Without the various corrections the two curves should be equal.

The measured values of the left-hand side of Eq. (49) show a quadratic behavior up to about $E = 2500$ V/cm.

We obtained

$$-\beta_{\langle 100\rangle} = (5\times 10^{-8} \pm 20\%)\ \mathrm{cm}^2/\mathrm{V}^2$$

and

$$-\beta_{\langle 110\rangle} = (2\times 10^{-8} \pm 30\%)\ \mathrm{cm}^2/\mathrm{V}^2$$

from measurements on four different devices for each orientation at a temperature of 77 °K. At 300 K the devices showed no deviations due to hot electrons up to $E = 2500$ V/cm within the accuracy of our measurements.

To compare the experimental results with the theory of Secs. II, III, and IV, we have to estimate the effect of the repopulation of higher valleys. The structure of subbands was given by Stern and Howard.[1] For our (110) inverted silicon surface

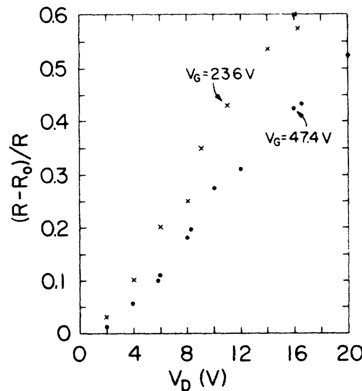

FIG. 3. Deviations from Ohm's law vs V_D for two different gate voltages. The measurements for each gate voltage have been performed with samples No. TE10-4a, TE10-4b, TE10-7, TE10-9 (Ref. 16).

there are four identical valleys (valleys with parallel main axes) at the lowest energy. The lines of equal energy are ellipses with masses along the main axes given in Table I. The subband next higher in energy contains two ellipsoidal valleys with the main axes perpendicular to the main axes of the lower ellipses. At 77 °K this subband contains about 5% of the total carrier concentration in thermal equilibrium. A calculation of the repopulation of the different subbands due to the warm-electron effect seems to be extremely difficult because of the following reasons:

(i) The energy distance of the subbands depends on the distribution function of the carriers.

(ii) The distribution function is most probably a very complicated function of energy as shown before.

One can, however, extract the repopulation effect out of the experiments making some plausible assumptions. Since the dominant scattering processes (acoustic phonons and surface roughness) do not depend on energy we can write for the conductivity

$$\sigma = e(\mu_1 n_1 + \mu_2 n_2) . \tag{51}$$

n_1 is the number of carriers and μ_1 the mobility of these carriers in the lowest valleys. n_2, μ_2 are the corresponding quantities for the higher valleys. Let Δn_1 be the change of the carrier concentration due to the electric field $\vec{E}$, and $n_{1,2}^0$, $\mu_{1,2}^0$ the carrier concentration and mobility for $\vec{E} = 0$. As mentioned before $n_2^0 \ll n_1^0$. Thus we can drop the field dependence of μ_2 as a higher-order effect. Doing this we obtain from (51)

$$\sigma = \sigma_0[1 + \beta^s E^2 + (\Delta n_1/n_1^0)(\mu_2^0/\mu_1^0 - 1)] . \tag{52}$$

β^s is the warm-electron coefficient for the lower valleys alone.

σ has been measured for two different orientations. Inserting these measured values in Eq. (52) we obtain two equations for the four unknowns $\beta^s_{\langle 100\rangle}$, $\beta^s_{\langle 110\rangle}$, $\Delta n_{1\langle 100\rangle}$, $\Delta n_{1\langle 110\rangle}$. The theoretical ratio of $\beta^s_{\langle 110\rangle}/\beta^s_{\langle 100\rangle}$ is given by 0.3435 from Eq. (35). This is the ratio of the mean energy deviation due to the field in the different direction. For the case of a Maxwellian distribution function with T_e, Δn_1 must also be proportional to this mean energy deviation. We can therefore also insert for $\Delta n_{1\langle 110\rangle}/\Delta n_{1\langle 100\rangle} = 0.3435$ with some justification. Doing this we obtain

$$\Delta n_{1\langle 100\rangle} = -11\,000\,[E(\mathrm{V/cm})]^2 . \tag{53}$$

This is a very small number and one can neglect the deviations from Ohm's law due to Eq. (52). Though this estimate is rather crude, the repopulation effect must be a minor effect in any case. Else the measured deviations from Ohm's law would have different sign in the different directions

since the main axes of the ellipses of the higher and lower valleys are perpendicular which was not observed.

As outlined earlier one has to know the electron-intervalley optical-phonon coupling constants Z_R for a comparison with the theory. There has been a great deal of uncertainty in the literature concerning these coupling constants.[20,21] It appears to be resolved now from symmetry considerations,[21,22] that there are two types of invervalley optical phonons in Si which are important for electron transport. We assume that both of them are f type (scattering between valleys on different axes) although there are some doubts of this fact. The Debye temperatures are $\Theta_1 = 670$ K and $\Theta_2 = 190$ K. According to Ref. 21 the coupling to the lower-energy phonons should be very small. We calculated β^s for the non-Maxwellian distribution of Fig. 1 with the data set 1 of Table I using one type of optical phonons only. β^s has also been evaluated for both types of optical phonons including impurity scattering but using a Maxwellian distribution function. Best fit was obtained in this case for data set 2 of Table I. The value for $\mu_{ac\,r}/\mu_I$ was obtained from measurements of the conductivity mobility vs the temperature as given in Ref. 2.

A summary of the results is given in Table II. Note that the two-dimensional β values are three orders of magnitude lower than the three-dimensional bulk value. This is due to the low mobility of the surface channel and to the fact that the two-dimensional momentum relaxation $\tau_{ac\,r}$ does not depend on energy. This is a further verification of the importance of the "two-dimensional model of scattering" at the surface.

As outlined, the values of the electron-intervalley optical-phonon coupling constants deduced, have to be regarded as qualitative only. Especially $Z_{670}(=Z_1)$ enters only weakly in the calculation because Θ_1 is so high. However, Z_{670} was already deduced from mobility measurements.[2] In addition, a large coupling constant Z_{670} is essential for the explanation of experiments in the hot-electron region.

Fang and Fowler[23] and Sato *et al.*[24] performed experiments in the hot-electron region using MOS transistors with extremely short channels. In their papers they gave results for a (100) inverted surface at room temperature. The lowest valleys for this orientation are two identical spheres with a density of states mass of $0.19m$. The next higher valleys are four equivalent ellipses with $m_t = 0.19m$ and $m_l = 0.91m$. As a consequence of the higher density of states mass of $0.416m$ and the larger number of valleys, they are preferably populated, especially as the carrier energy is higher in the high field. Therefore, we took into account only these valleys for a comparison of the experiments with the theory.

The electron concentration in their experiments was about $6\times10^{12}/\text{cm}^2$. We can expect therefore that electron-electron scattering is effective and that a Maxwellian distribution at T_e will give semiquantitative results.

Figure 4 shows the result of calculations using Eqs. (43)–(47) and data set 1. The two full curves are calculated for a (100) surface and $\langle 110\rangle$ and $\langle 010\rangle$ channel directions. The dashed line is experimental. The choice of a high electron-intervalley optical phonon coupling constant Z_1 is essential, whereas $Z_{190}(=Z_2)$ enters the calculation now very weakly since Θ_2 is small and this type of optical scattering becomes essentially independent of energy at higher electron temperatures.

Again, of course, the calculations are only semiquantitative. Deviation of theory from experiment at the highest field strength, as the electron tem-

TABLE II. Values of β for a (110) surface and $\langle 110\rangle$ channel directions.

		$-\beta_{\langle 100\rangle}$	$-\beta_{\langle 110\rangle}$	$-\beta^s_{\langle 100\rangle}$ (cm^2/V^2)	$-\beta^s_{\langle 110\rangle}$	$\Delta n_{1\langle 100\rangle}$ (cm^{-2})
Theory	Maxwellian data set 1			3.2×10^{-8}	1.1×10^{-8}	
	Maxwellian data set 2			5.7×10^{-8}	2.0×10^{-8}	
	Non-Maxwellian data set 1			1.8×10^{-7}	6.2×10^{-8}	
Experiment		$(5.0\pm1)\times10^{-8}$	$(2.0\pm0.6)\times10^{-8}$			$-11\,000[E(\text{V/cm})]^2$ [see Eq. (53)]
Bulk[a]		$-\beta_{\langle 111\rangle}=1\times10^{-5}$ cm^2/V^2				

[a]Experimental bulk value in n-Si at 77 °K for a small amount of impurity scattering with $\vec{E}$ in the $\langle 111\rangle$ direction. See Ref. 20.

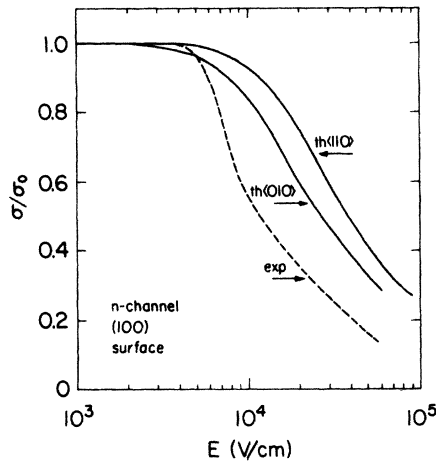

FIG. 4. Conductivity for electrons on a (100) surface and ⟨010⟩ and ⟨110⟩ direction of the current vs electric field: ———— theoretical; - - experimental, j parallel ⟨110⟩.

perature goes up to 2000 °K, is expected and is caused by transitions between the two-dimensional subbands which restore the distribution to the three-dimensional case.

VI. CONCLUSION

We presented experiments showing that the value of the warm electron coefficient β for n-inverted silicon surface layers is of the order 10^{-8} cm^2/V^2 whereas for the bulk case it is 10^{-5} cm^2/V^2. We have been able to explain this large discrepancy, as well as the hot-carrier effects measured by Fang and Fowler, by a two-dimensional theory. The electron-phonon coupling constants used lie well in the range of coupling constants given in the literature for bulk n-silicon and close to a set of constants given recently.[21]

Electron scattering by intervalley optical phonons and ionized impurities are the only mechanisms which depend on energy for a two-dimensional carrier gas. The deviations from Ohm's law are therefore governed by optical scattering alone if impurity scattering is unimportant, in contrast to the three-dimensional case, where scattering by acoustic phonons plays an important role. One can therefore expect that the coupling constants obtained in this paper are more significant than coupling constants obtained from a similar experiment for bulk n-Si using a Maxwellian distribution function. However, we would rather like to stress here the qualitative nature of the Maxwellian approach, than enriching the literature with an additional set of Z_R.

For the two-dimensional case, we were able to give explicit formulas for non-Maxwellian distribution functions, while it could be obtained only numerically in the three-dimensional case. The similarity and differences between solutions for the two- and three-dimensional case are given in the Appendix.

ACKNOWLEDGMENTS

We would like to thank Dr. J. R. Edwards, now at Bell Laboratories, for the use of the field-effect devices he fabricated in our laboratory, Dr. T. H. Ning, now at IBM Research Lab, Yorktown Heights, N.Y., for helpful discussions during the earlier stage of this work, and Tung Chu for construction of the measurement circuits. We wish to thank Dr. F. Stern for the preprints he sent us which were referenced in the text. One of the authors (K.H.) would also like to thank Professor W. Philipp and Professor E. Scott of the mathematics department for valuable discussions concerning the solutions of Eq. (17). He would also like to acknowledge a travel grant received from the Fulbright-Hays Committee.

APPENDIX

Neglecting the absorption term, the three-dimensional form of Eq. (25) is[11]

$$\frac{d}{dx}(xe^{-x}) = \frac{d}{dx}\left(e^{-x}x^2\frac{d\xi}{dx}\right) + (S_R/S_A)\,x^{1/2}e^{-x}(N_R+1)(x-x_R)^{1/2} \times [\xi(x-x_R)-\xi(x)]\,. \quad \text{(A1)}$$

For $0 \le x < x_R$ Eq. (A1) reduces to

$$\frac{d}{dx}(xe^{-x}) = \frac{d}{dx}\left(e^{-x}x^2\frac{d\xi}{dx}\right)\,.$$

The solution is

$$\xi(x) = \ln x + b_1\,, \quad \text{(A2)}$$

For $x_R \le x < 2x_R$ Eq. (A1) reads

$$\frac{d}{dx}(xe^{-x}) = \frac{d}{dx}\left(e^{-x}x^2\frac{d\xi}{dx}\right) + (S_R/S_A)\,x^{1/2}e^{-x}(N_R+1)(x-x_R)^{1/2} \times[\xi(x-x_R)-\xi(x)]\,. \quad \text{(A3)}$$

(A3) cannot be solved as easily as the corresponding Eq. (28) because of the cumbersome square roots. For a high S_R/S_A ratio, however, one can rewrite (A3) as

$$\xi(x-x_R) - \xi(x) = 0 \quad \text{(A4)}$$

neglecting the other terms. One can find by inspection that this approximation is good for some x^* such that $x > x^*$. For $S_R/S_A = 300$ we obtained $x^* \simeq 1.1x_R$. Thus the distribution function becomes

$$\xi(x) = \ln(x-x_R) + b_1 \quad \text{(A5)}$$

for $x^* \leq x \leq 2x_R$.

As we can see from Eqs. (A2) and (A5), the distribution function must have a distinct step at $x = x_R$ so that the number of electrons above x_R is considerably lower than that in a Maxwellian approximation. Furthermore, it can easily be seen that a polynomial approximation, as used in the variational method of Adawi,[11] will converge slowly. Adawi expanded $\xi(x)$ as

$$\xi(x) = \sum_r c_r[x^r - (\tfrac{3}{2})(\tfrac{5}{2}) \cdots (2r+1)/2] .$$

We calculated the variation polynomial coefficients c_r up to $r = 14$ for $S_R/S_A = 300$ and $x_R = 5$. The term proportional to c_{10} still gave large contributions to $\xi(x)$ for $x > x_R$.[25]

*Supported by the Air Force Office of Scientific Research, Grant No. AFOSR-71-2067, the Advanced Research Projects Agency, and the National Science Foundation, Grant No. GK30283.

†On leave of absence from the Institut für Angewandte Physik, University of Vienna, and the Ludwig-Boltzmann Institut für Festkörperphysik, Vienna, Austria.

[1]F. Stern and W. E. Howard, Phys. Rev. 163, 816 (1967).

[2]C. T. Sah, T. H. Ning, and L. L. Tschopp, Surf. Sci. 32, 561 (1972).

[3]E. M. Conwell, in *Solid State Physics*, edited by F. Seitz, D. Turnbull and H. Ehrenreich (Academic, New York, 1967), Suppl. 9.

[4]T. N. Morgan, J. Phys. Chem. Solids 8, 245 (1959).

[5]D. K. Ferry, Phys. Rev. B 8, 1544 (1973).

[6]H. Frohlich and B. V. Paranjape, Proc. Phys. Soc. Lond. B 69, 21 (1956).

[7]F. Stern, J. Vac. Sci. Tech. 9, 752 (1972).

[8]C. T. Sah, Bull. Amer. Phys. Soc. Ser. IV 18, 394 (1973).

[9]Theoretical results for the scattering of channel electrons via the deformation potential of acoustical phonons have been given by (K1) S. Kawaji, J. Phys. Soc. Jpn. 27, 906 (1969); (K2) S. Kawaji (private communication, November, 1972); (E1) H. Ezawa, Toshio Kuroda, and Koichi Nakamura, Surf. Sci. 24, 654 (1971); (E2) H. Ezawa, S. Kawaji, T. Kuroda, and K. Nakamura, Surf. Sci. 24, 659 (1971).

[10]T. H. Ning and C. T. Sah, Phys. Rev. B 6, 4605 (1972).

[11]I. Adawi, Phys. Rev. 120, 118 (1960).

[12]In the formalism used by Ferry in Ref. 5 the neglecting of the abosprtion is more problematic since the distribution function must be Maxwellian for $E = 0$. This is fulfilled automatically in our case because of the expansion in Eq. (20).

[13]H. D. Rees, J. Phys. Chem. Solids 30, 643 (1969).

[14]A. D. Boardman, W. Fawcett, and H. D. Rees, Solid State Commun. 6, 305 (1968).

[15]H. Heinrich and M. Kriechbaum, J. Phys. Chem. Solids 31, 927 (1970).

[16]J. R. Edwards, Ph.D. thesis (University of Illinois, Urbana, Illinois, 1969) (unpublished).

[17]C. T. Sah, J. R. Edwards, and T. H. Ning, Phys. Status Solidi (A) 10, 153 (1972).

[18]Equation (48) has been derived as outlined in a paper by C. T. Sah and H. C. Pao [IEEE Trans. Electron Devices ED-13, 393 (1966)] replacing the mobility μ by $\mu[1 + \beta E^2 + (\partial\mu/\partial V_G) V(y)/\mu]$. We used the same notation as Sah and Pao.

[19]F. Stern, Crit. Rev. in Solid State Sci. (to be published).

[20]M. Costato, S. Fontanesi, and L. Reggiani, J. Phys. Chem. Solids 34, 547 (1973).

[21]P. Norton, T. Braggins, and H. Levinstein, Phys. Rev. B (to be published).

[22]M. Lax and J. L. Briman, Phys. Status Solidi (B), 49, K153 (1972).

[23]F. F. Fang and A. B. Fowler, J. Appl. Phys. 41, 1825 (1969).

[24]T. Sato, Y. Takeisiki, H. Tango, H. Ohnuma, and Y. Okamoto, J. Phys. Soc. Jpn. 31, 1846 (1971).

[25]These calculations have been performed at the Ludwig Boltzmann Institut für Festkörperphysik in 1969.